09

Four-wave mixing by mixed holograms in the photorefractive crystal of 23 symmetry class

© V.N. Naunyka

Mozyr State Pedagogical University named after I.P.Shamyakin,
247760 Mozyr, Republic of Belarus
e-mail: valnav@inbox.ru

Received July 18, 2024
Revised August 18, 2024
Accepted August 22, 2024

The results of a theoretical study of the laws of degenerate four-wave mixing in a cubic photorefractive crystal of 23 symmetry class are presented. When obtaining the coupled waves equations, it was assumed that light beams have linear polarization, and six mixed holographic gratings are recorded in the crystal. The theoretical model takes into account linear electro-optical, inverse piezoelectric and photoelastic effects, as well as optical activity, natural absorption and circular dichroism of the crystal. The dependences of the reflection coefficient on the thickness of the crystal and the azimuth of the linear polarization of light beams are analyzed for cases when amplitude, phase and mixed gratings are recorded in the crystal by four-wave mixing. It has been established that the highest value of the azimuth-optimized polarization intensity of the phase-conjugated light beam is achieved by diffraction by mixed gratings. The combinations of crystal thickness and light beam polarization azimuths at which maximum values of the reflection coefficient are achieved are determined. It is shown that the efficiency of diffraction of light beams by mixed holographic grating depends on the magnitude of its spatial shift relative to the recording interference pattern.

Keywords: Photorefractive crystal, four-wave mixing, reflection coefficient, optical activity, azimuth of polarization.

DOI: 10.61011/TP.2024.11.59751.212-24

Introduction

A volume mixed hologram is a set of phase and amplitude holographic gratings (hereinafter — gratings), which are formed by modulating the refractive index and absorption coefficient of the recording medium [1]. The possibility of recording mixed (phase-amplitude) gratings in a photorefractive crystal of the $\bar{4}3m$ symmetry class was experimentally demonstrated in Ref. [2]. It was found that the appearance of phase and amplitude gratings is attributable to a single process of formation of the electric field of spatially separated charges in a photorefractive crystal. It is shown in this paper that the formation of an amplitude grating can have a significant effect on the efficiency of light wave diffraction.

The fundamental principles of the degenerate four-wave mixing (FWM) on photoinduced gratings recorded in recording materials by interfering waves are systematically described and generalized in Ref. [3]. Special attention is paid in this paper to the description of the physics of the process of light amplification, which takes place as a result of energy exchange between light waves during their self-diffraction on dynamic gratings recorded in a nonlinear medium. Most of studies (see, for example, [4,5]) analyze the patterns of FWM without taking into account optical activity. The results obtained in such studies can be used to study the features of the wavefront conjugation (WFC) in photorefractive crystals of the $\bar{4}3m$ symmetry class. A number of papers have also been published (see, for example, [6,7]), in which the theory of FWM is presented taking into account optical activity and can be applied in the case when a photorefractive crystal of 23 symmetry class is used as a recording nonlinear medium. The above studies when solving the coupled waves equations did not take into account the additional modulation of the dielectric constant of the recording medium at optical frequencies as a result of the mixed action of photoelastic and inverse piezoelectric effects, which are inherent in cubic crystals. A brief overview of theoretical and experimental studies of the photorefractive effect and properties of volume holograms in cubic optically active piezocrystals is presented in Ref. [8].

Currently, the features of diffraction and mixing of light beams on dynamic gratings in photorefractive crystals are studied by a number of research groups. The scientific traditions laid down in the pioneering study of the phase conjugation of light beams at FWM [9] are supported and multiplied by Belarusian scientists. Modern papers study the dynamics of photoinduced absorption and conditions for recording photorefractive gratings in crystals of the sillenite family[10]. The authors experimentally demonstrated that there are two mechanisms for recording gratings in a $Bi_{12}TiO_{20}$ (BTO) crystal in case of usage of nanosecond laser pulses with an intensity of the order of 1 MW/cm^2.

Spectral patterns of recording short- and long-lived gratings in a BTO crystal were defined by non-contact diagnostics using dynamic holography [11]. The obtained results will be useful for application of bismuth titanate crystals in adaptive holographic interferometry systems.

A fundamental contribution to the development of photorefractive crystal optics and the wavefront conjugation theory was made by the Tomsk Scientific Group (see, for example, [12]). The conditions for the generation of WFC in $Bi_{12}SiO_{20}$ (BSO) and BTO samples were determined in Ref. [13] with the orientation of the grating vector along the direction $[\bar{1}10]$ and arbitrary linear polarization of light waves propagating in the plane (001). The possibility of effective WFC on reflection phase gratings in a crystal BTO:Fe, Cu in case of a diffusion mechanism of charge separation without the application of an external electric field is demonstrated in Ref. [14]. The authors present a system of coupled wave equations suitable for describing the contra-directional mixing in a crystal of arbitrary cross-section, which take into account the mixed effect of linear electro-optical, photoelastic and inverse piezoelectric effects, as well as optical activity and absorption of the recording medium. A number of interesting results have been presented in recent publications of the scientific group. The dependences of the signal beam amplitude on the frequency of phase modulation of light, intensity and spatial frequency of the interference pattern were studied in Ref. [15] and photoelectric characteristics of a lithium niobate crystal were determined as a result of the studies. The possibility of creating photovoltaic tweezers for the formation of volume transmission holograms in a lithium niobate crystal with diffusion alloying with copper is considered in Ref. [16].

The priority scientific results and original developments in the field of using nonlinear photorefractive crystals to control optical radiation, consistently presented in the monograph [17], were obtained by St. Petersburg scientists. The authors consider the fundamental principles of the theory of interference and diffraction of light beams on dynamic photorefractive gratings formed in nonlinear media. The practical aspects of usage of photorefractive crystals to create a component base of modern optical and information systems (adaptive holographic interferometers, integrated optical modulators, controlled diffraction gratings, optical radiation filters, etc.) are considered.

Despite a sufficient number of studies of the FWM patterns on photoinduced gratings in cubic photorefractive crystals, the results obtained in most studies are valid for fixed values of crystal thickness, azimuths of polarization of light waves, orientation angles of the crystal, spatial shifts between induced interference patterns and holographic gratings (hereinafter — spatial shift). It is of interest to study the more general case when the reflectance is a function of several parameters at a time (for example, crystal thickness, polarization azimuths, etc.) and to determine the optimal conditions of a holographic experiment under which the highest WFC efficiency is achieved. It is useful to consider cases when several gratings with a phase-amplitude structure are formed simultaneously in a crystal. Solving such a problem will allow determining the dependence of the intensity of the phase-conjugated light wave on the thickness of the crystal and the azimuth of polarization of light waves with a greater accuracy, as well as predicting methods to increase the efficiency of diffraction in FWM by controlling the characteristics of a holographic system. The results of such a study are partially presented in a short report in Ref. [18], in which the dependence of the azimuth-optimized linear polarization of light waves of the reflectance values at the contra-directional FWM on the thickness of the BSO crystal of (001)-cut was studied. These data allow determining the thickness of the crystal at which the highest reflectance is achieved. However, the paper did not consider the issue of the azimuths of polarization of the light waves entering the crystal, at which the greatest intensity of the phase-conjugated wave is achieved, and the diffraction contributions of the phase and amplitude components of the mixed grating at WFC were not analyzed.

The patterns of simultaneous diffraction and energy exchange between linearly polarized light beams at FWM on mixed photorefractive gratings recorded in an optically active absorbing piezocrystal are studied in this paper. A system of differential equations has been obtained that can be used to find the polarization components of light beams and analyze the patterns of WFC in a cubic photorefractive crystal of 23 symmetry class. The numerical solution of the obtained results was used to find the values of the crystal thickness and the polarization azimuth of the light beams at the input to the crystal at which the intensity of the phase-conjugated light beam at FWM will reach the highest value. We performed a comparative analysis of the dependencies of the maximum and minimum reflectance values on the crystal thickness calculated for cases when phase, amplitude and mixed gratings are formed in a cubic photorefractive crystal.

1. Theoretical model

Figure 1 shows the scheme of mixing of linearly polarized pump beams 1, 2 and a signal beam 3 in a photorefractive crystal of 23 symmetry class, a detailed description of which is given in Ref. [19]. Two transmission and four reflection gratings [3] can be recorded in a nonlinear medium in case of FWM according to the scheme shown in Fig. 1, *a*. The light beams 1–3 determine the recording of three primary gratings: the transmission grating 13 is formed as a result of the mixing of beams 1 and 3, and the reflection gratings 12 and 23 are formed by pairwise interference of beams 1, 2 and 2, 3. Self-diffraction of beams on primary gratings changes their amplitude-phase characteristics and results in the appearance of

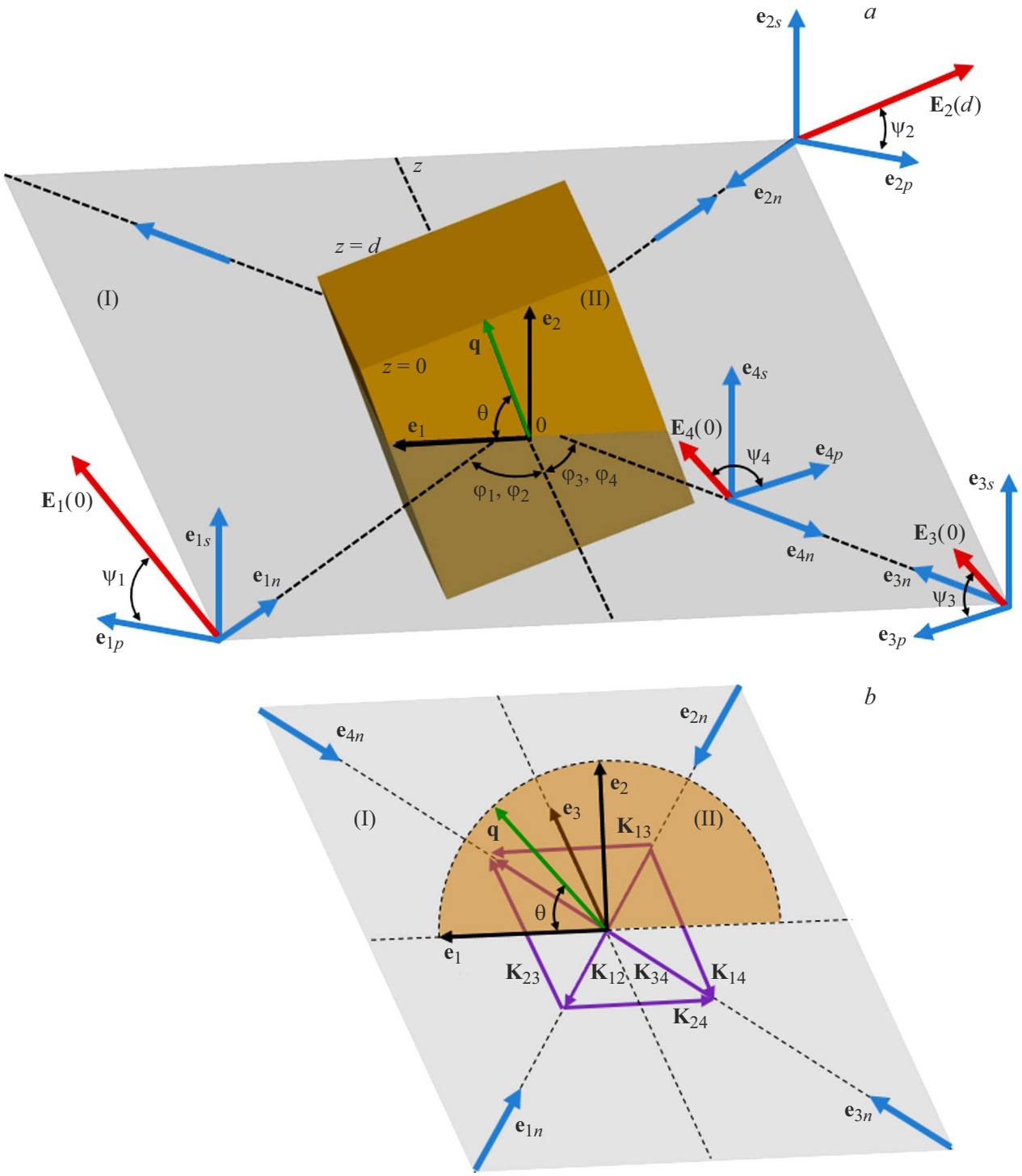

Figure 1. Geometric scheme of the four-wave mixing in a photorefractive crystal (*a*); orientation of the wave vectors of holographic gratings in the plane of incidence (*b*).

a phase-conjugated beam 4. The interference of this beam with beams 1–3 leads to the recording of three secondary gratings: the transmission grating 24 and two reflection gratings 14, 34. The location of the wave vectors of the primary and secondary gratings in the plane of incidence is shown in Fig. 1, *b*. It is well known (see, for example, [20]) that the efficiency of WFC is determined by the spatial orientation of a cubic crystal, the mutual spatial shift of photorefractive gratings and the azimuths of polarization of light beams. These factors are taken into account in the theoretical model by using the following assumptions for deriving equations: the

amplitudes and phases of recording light beams change in case of their self-diffraction on recorded gratings; the crystal is arbitrarily oriented in space relative to the plane of incidence; six mixed gratings with arbitrary spatial shifts relative to the corresponding interference patterns are recorded in a nonlinear medium; linearly polarized light beams have arbitrary azimuth values ψ_j at the input to the crystal.

The wave equation for optically active absorbing media in the approximation of slowly varying amplitudes and smallness of the Bragg angle φ_B can be represented as follows:

$$\begin{aligned}\frac{dE_{1p}}{dz} =& m_{12}[(ie^{i\delta_{12}}\kappa_{1p2p} - e^{i\phi_{12}}\sigma_{1p2p})E_{2p} \\ &+(ie^{i\delta_{12}}\kappa_{1p2s} - e^{i\phi_{12}}\sigma_{1p2s})E_{2s}] \\ &+m_{13}[(ie^{i\delta_{13}}\kappa_{1p3p} - e^{i\phi_{13}}\sigma_{1p3p})E_{3p} \\ &+(ie^{i\delta_{13}}\kappa_{1p3s} - e^{i\phi_{13}}\sigma_{1p3s})E_{3s}] \\ &+m_{14}[(ie^{i\delta_{14}}\kappa_{1p4p} - e^{i\phi_{14}}\sigma_{1p4p})E_{4p} \\ &+(ie^{i\delta_{14}}\kappa_{1p4s} - e^{i\phi_{14}}\sigma_{1p4s}E_{4s}] \\ &+(\rho_1 + i\chi_1)E_{1s} - \alpha_1 E_{1p},\end{aligned}$$

$$\begin{aligned}\frac{dE_{1s}}{dz} =& m_{12}[(ie^{i\delta_{12}}\kappa_{1s2p} - e^{i\phi_{12}}\sigma_{1s2p})E_{2p} \\ &+(ie^{i\delta_{12}}\kappa_{1s2s} - e^{i\phi_{12}}\sigma_{1s2s})E_{2s}] \\ &+m_{13}[(ie^{i\delta_{13}}\kappa_{1s3p} - e^{i\phi_{13}}\sigma_{1s3p})E_{3p} \\ &+(ie^{i\delta_{13}}\kappa_{1s3s} - e^{i\phi_{13}}\sigma_{1s3s})E_{3s}] \\ &+m_{14}[(ie^{i\delta_{14}}\kappa_{1s4p} - e^{i\phi_{14}}\sigma_{1s4p})E_{4p} \\ &+(ie^{i\delta_{14}}\kappa_{1s4s} - e^{i\phi_{14}}\sigma_{1s4s})E_{4s}] \\ &-(\rho_1 + i\chi_1)E_{1p} - \alpha_1 E_{1s},\end{aligned}$$

$$\begin{aligned}\frac{dE_{2p}}{dz} =& m_{12}^*[(ie^{-i\delta_{12}}\kappa_{2p1p} - e^{-i\phi_{12}}\sigma_{2p1p})E_{1p} \\ &+(ie^{-i\delta_{12}}\kappa_{2p1s} - e^{-i\phi_{12}}\sigma_{2p1s})E_{1s}] \\ &+m_{23}[(ie^{i\delta_{23}}\kappa_{2p3p} - e^{i\phi_{23}}\sigma_{2p3p})E_{3p} \\ &+(ie^{i\delta_{23}}\kappa_{2p3s} - e^{i\phi_{23}}\sigma_{2p3s})E_{3s}] \\ &+m_{24}[(ie^{i\delta_{24}}\kappa_{2p4p} - e^{i\phi_{24}}\sigma_{2p4p})E_{4p} \\ &+(ie^{i\delta_{24}}\kappa_{2p4s} - e^{i\phi_{24}}\sigma_{2p4s})E_{4s}] \\ &+(\rho_2 + i\chi_2)E_{2s} - \alpha_2 E_{2p},\end{aligned}$$

$$\begin{aligned}\frac{dE_{2s}}{dz} =& m_{12}^*[(ie^{-i\delta_{12}}\kappa_{2s1p} - e^{-i\phi_{12}}\sigma_{2s1p})E_{1p} \\ &+(ie^{-i\delta_{12}}\kappa_{2s1s} - e^{-i\phi_{12}}\sigma_{2s1s})E_{1s}] \\ &+m_{23}[(ie^{i\delta_{23}}\kappa_{2s3p} - e^{i\phi_{23}}\sigma_{2s3p})E_{3p} \\ &+(ie^{i\delta_{23}}\kappa_{2s3s} - e^{i\phi_{23}}\sigma_{2s3s})E_{3s}] \\ &+m_{24}[(ie^{i\delta_{24}}\kappa_{2s4p} - e^{i\phi_{24}}\sigma_{2s4p})E_{4p} \\ &+(ie^{i\delta_{24}}\kappa_{2s4s} - e^{i\phi_{24}}\sigma_{2s4s})E_{4s}] \\ &-(\rho_2 + i\chi_2)E_{2p} - \alpha_2 E_{2s},\end{aligned}$$

$$\begin{aligned}\frac{dE_{3p}}{dz} =& m_{13}^*[(ie^{-i\delta_{13}}\kappa_{3p1p} - e^{-i\phi_{13}}\sigma_{3p1p})E_{1p} \\ &+(ie^{-i\delta_{13}}\kappa_{3p1s} - e^{-i\phi_{13}}\sigma_{3p1s})E_{1s}] \\ &+m_{23}^*[(ie^{-i\delta_{23}}\kappa_{3p2p} - e^{-i\phi_{23}}\sigma_{3p2p})E_{2p} \\ &+(ie^{-i\delta_{23}}\kappa_{3p2s} - e^{-i\phi_{23}}\sigma_{3p2s})E_{2s}] \\ &+m_{34}[(ie^{i\delta_{34}}\kappa_{3p4p} - e^{i\phi_{34}}\sigma_{3p4p})E_{4p} \\ &+(ie^{i\delta_{34}}\kappa_{3p4s} - e^{i\phi_{34}}\sigma_{3p4s})E_{4s}] \\ &+(\rho_3 + i\chi_3)E_{3s} - \alpha_3 E_{3p},\end{aligned}$$

$$\begin{aligned}\frac{dE_{3s}}{dz} =& m_{13}^*[(ie^{-i\delta_{13}}\kappa_{3s1p} - e^{-i\phi_{13}}\sigma_{3s1p})E_{1p} \\ &+(ie^{-i\delta_{13}}\kappa_{3s1s} - e^{-i\phi_{13}}\sigma_{3s1s})E_{1s}] \\ &+m_{23}^*[(ie^{-i\delta_{23}}\kappa_{3s2p} - e^{-i\phi_{23}}\sigma_{3s2p})E_{2p} \\ &+(ie^{-i\delta_{23}}\kappa_{3s2s} - e^{-i\phi_{23}}\sigma_{3s2s})E_{2s}] \\ &+m_{34}[(ie^{i\delta_{34}}\kappa_{3s4p} - e^{i\phi_{34}}\sigma_{3s4p})E_{4p} \\ &+(ie^{i\delta_{34}}\kappa_{3s4s} - e^{i\phi_{34}}\sigma_{3s4s})E_{4s}] \\ &-(\rho_3 + i\chi_3)E_{3p} - \alpha_3 E_{3s}\end{aligned}$$

$$\begin{aligned}\frac{dE_{4p}}{dz} =& m_{14}^*[(ie^{-i\delta_{14}}\kappa_{4p1p} - e^{-i\phi_{14}}\sigma_{4p1p})E_{1p} \\ &+(ie^{-i\delta_{14}}\kappa_{4p1s} - e^{-i\phi_{14}}\sigma_{4p1s})E_{1s}] \\ &+m_{24}^*[(ie^{-i\delta_{24}}\kappa_{4p2p} - e^{-i\phi_{24}}\sigma_{4p2p})E_{2p} \\ &+(ie^{-i\delta_{24}}\kappa_{4p2s} - e^{-i\phi_{24}}\sigma_{4p2s})E_{2s}] \\ &+m_{34}^*[(ie^{-i\delta_{34}}\kappa_{4p3p} - e^{-i\phi_{34}}\sigma_{4p3p})E_{3p} \\ &+(ie^{-i\delta_{34}}\kappa_{4p3s} - e^{-i\phi_{34}}\sigma_{4p3s})E_{3s}] \\ &+(\rho_4 + i\chi_4)E_{4s} - \alpha_4 E_{4p},\end{aligned}$$

$$\frac{dE_{4s}}{dz} = m_{14}^{*}[(ie^{-i\delta_{14}}\kappa_{4s1p} - e^{-i\phi_{14}}\sigma_{4s1p})E_{1p} + (ie^{-i\delta_{14}}\kappa_{4s1s} - e^{-i\phi_{14}}\sigma_{4s1s})E_{1s}] + m_{24}^{*}[(ie^{-i\delta_{24}}\kappa_{4s2p} - e^{-i\phi_{24}}\sigma_{4s2p})E_{2p} + (ie^{-i\delta_{24}}\kappa_{4s2s} - e^{-i\phi_{24}}\sigma_{4s2s})E_{2s}] + m_{34}^{*}[(ie^{-i\delta_{34}}\kappa_{4s3p} - e^{-i\phi_{34}}\sigma_{4s3p})E_{3p} + (ie^{-i\delta_{34}}\kappa_{4s3s} - e^{-i\phi_{34}}\sigma_{4s3s})E_{3s}] - (\rho_4 + i\chi_4)E_{4p} - \alpha_4 E_{4s}.$$

The following symbols and notations are used here: $\kappa_{hbut} = (\kappa_0(e_{hb}\Delta\hat{b}_{hu}e_{ut}))/\cos\varphi_h$, $\sigma_{hbut} = (\sigma_0(e_{hb}\Delta\hat{\sigma}_{hu}e_{ut}))/\cos\varphi_h$, $\rho_h = \rho/\cos\varphi_h$, $\chi_h = \chi/\cos\varphi_h$, $\alpha_h = \alpha/\cos\varphi_h$, where $\kappa_0 = \pi n_0^3/(2\lambda)$ — the coupling constant of the phase component of the grating, $\sigma_0 - \pi/(nc)$ — coupling constant of the amplitude component of the grating, $\delta\hat{b}_{hu}$ — change in the inverse dielectric constant of the crystal, $\Delta\hat{\sigma}_{hu}$ — change in the conductivity tensor of the crystal, φ_h — Bragg angle in the incidence plane for the beam h, δ_{hu} and ψ_{hu} — spatial shifts of the phase and amplitude components of the recorded grating hu relative to the recording interference pattern hu, n_0 — refractive index of an undisturbed crystal, ρ — specific rotation, α — linear absorption coefficient, χ — circular dichroism parameter, λ — wavelength, c — speed of light in vacuum, i — imaginary unit. When considering the indices h and u, it should be borne in mind that if they do not stand side by side (for example, κ_{hbut}), they should be attributed to the designation of the light beam: 1, 2, 3 or 4. If the indexes h and u are located side by side (for example, $\Delta\hat{b}_{hu}$), then the index hu corresponds to the grid number, which can have one of the following values: 12, 13, 14, 23, 24, 34. The indices b and t denote p- or s-components of the beames.

The variables E_{hp} and E_{hs} are the polarization components of the light beam h in the coupled wave equations, which are equal to the projections of the electric field intensity vector E_h on the axis coinciding in the direction with the unit vectors $\mathbf{e}_{hp}$ and $\mathbf{e}_{hs}$. The variable m_{hu} indicates the modulation depth of the recording interference pattern hu, which is found using the formula: $m_{hu} = (E_{hs}E_{us} + E_{hp}E_{up}\cos(e_{hp}e_{up}))/I_0$, where $(e_{hp}e_{up})$ — the scalar product of the unit vectors e_{hp} and e_{up}, I_0 — the resulting intensity of the light field inside the crystal ($I_0 = E_{1p}^2 + E_{1s}^2 + E_{2p}^2 + E_{2s}^2 + E_{3p}^2 + E_{3s}^2 + E_{4p}^2 + E_{4s}^2$). The asterisk above the variable m_{hu} means complex conjugation. The physical meaning of the terms $(i\exp(i\delta_{hu})\kappa_{hbut} - \exp(i\phi_{hu})\sigma_{hbut})E_{ut}$ is to specify the relationship between the components E_{hb} and E_{ut} of light beams h and u when they are diffracted on the phase and amplitude components of the mixed grating hu respectively. Tensor convolutions $(e_{hb}\Delta\hat{b}_{hu}e_{ut})$ and $(e_{hb}\Delta\sigma_{hu}e_{ut})$ in variables κ_{hbut} and σ_{hbut} correspond to the values of diffraction contributions of the phase and amplitude components of the mixed grating hu during the formation of the phase-conjugated beam. The products $\rho_h E_{hp}$ and $\rho_h E_{hs}$ are used to find the increments of the variables E_{hp} and E_{hs}, which occurs due to rotation of the polarization plane of the light beam h when it propagates in optically active crystal. The terms $i\chi_h E_{hp}$ and $i\chi_h E_{hs}$ appear in the coupled wave equations due to the circular dichroism inherent in photorefractive crystals of 23 symmetry class [21], manifested in the difference of the absorption coefficients for components E_{hp} and E_{hs}. The products $\alpha_h E_{hp}$ and $\alpha_h E_{hs}$ are used to find changes in the components E_{hp} and E_{hs} with a decrease of the intensity of the light beam h under the effect of linear absorption of the crystal.

The change of the conductivity tensor $\Delta\hat{\sigma}_{hu}$ of the crystal in a linear contrast approximation is determined from the expression: $\Delta\hat{\sigma}_{hu} = m_{hu}\sigma_{hu}\delta_{kf}$, where σ_{hu} — conductivity coefficients, δ_{kf} — a unit symmetric tensor of the second rank. The components of the inverse dielectric constant tensor $\Delta\hat{b}_{hu}$ of the crystal will be found based on the well-known expressions [22]:

$$b_{11} = p_1 n_1 R_1 + p_2 n_2 R_2 + p_3 n_3 R_3,$$
$$b_{22} = p_1 n_2 R_2 + p_2 n_3 R_3 + p_3 n_1 R_1,$$
$$b_{33} = p_1 n_3 R_3 + p_2 n_1 R_1 + p_3 n_2 R_2,$$
$$b_{12} = b_{21} = p_4(n_1 R_2 + n_2 R_1) + r_{41} n_3,$$
$$b_{13} = b_{31} = p_4(n_1 R_3 + n_3 R_1) + r_{41} n_2,$$
$$b_{23} = b_{32} = p_4(n_2 R_3 + n_3 R_2) + r_{41} n_1,$$
$$R_1 = \gamma_{11} Q_1 + \gamma_{12} Q_2 + \gamma_{13} Q_3,$$
$$R_2 = \gamma_{21} Q_1 + \gamma_{22} Q_2 + \gamma_{23} Q_3,$$
$$R_3 = \gamma_{31} Q_1 + \gamma_{32} Q_2 + \gamma_{33} Q_3,$$
$$\gamma_{11} = (\Gamma_{22}\Gamma_{33} - \Gamma_{23}^2)/D,$$
$$\gamma_{22} = (\Gamma_{11}\Gamma_{33} - \Gamma_{13}^2)/D,$$
$$\gamma_{33} = (\Gamma_{11}\Gamma_{22} - \Gamma_{12}^2)/D,$$
$$\gamma_{12} = \gamma_{21} = (\Gamma_{13}\Gamma_{23} - \Gamma_{12}\Gamma_{33})/D,$$
$$\gamma_{13} = \gamma_{31} = (\Gamma_{12}\Gamma_{23} - \Gamma_{13}\Gamma_{22})/D,$$
$$\gamma_{23} = \gamma_{32} = (\Gamma_{12}\Gamma_{13} - \Gamma_{11}\Gamma_{23})/D,$$
$$D = \Gamma_{11}(\Gamma_{22}\Gamma_{33} - \Gamma_{23}^2) - \Gamma_{22}\Gamma_{13}^2 - \Gamma_{33}\Gamma_{12}^2 + 2\Gamma_{12}\Gamma_{13}\Gamma_{23}$$
$$\Gamma_{11} = c_1 n_1^2 + c_3(n_2^2 + n_3^2),$$
$$\Gamma_{22} = c_1 n_2^2 + c_3(n_1^2 + n_3^2),$$
$$\Gamma_{33} = c_1 n_3^2 + c_3(n_1^2 + n_2^2),$$
$$\Gamma_{12} = \Gamma_{21} = n_1 n_2(c_2 + c_3),$$
$$\Gamma_{13} = \Gamma_{31} = n_1 n_3(c_2 + c_3),$$
$$\Gamma_{23} = \Gamma_{32} = n_2 n_3(c_2 + c_3),$$
$$Q_1 = 2e_{14} n_2 n_3, \quad Q_2 = 2e_{14} n_1 n_3, \quad Q_3 = 2e_{14} n_1 n_2.$$

The following designations are used for nonzero components of linear electro-optical tensors ($\hat{r}^S$), photoelastic ($\hat{p}^E$) and inverse piezoelectric ($\hat{e}$) effects, as well as components of the elasticity tensor ($\hat{c}^E$):

$$r^S_{123} = r^S_{132} = r^S_{213} = r^S_{231} = r^S_{312} = r^S_{321} \equiv r_{41},$$

$$e_{123} = e_{132} = e_{213} = e_{231} = e_{312} = e_{321} \equiv e_{14},$$

$$c^E_{11} = c^E_{22} = c^E_{33} \equiv c_1,$$

$$c^E_{12} = c^E_{13} = c^E_{23} = c^E_{21} = c^E_{31} = c^E_{32} \equiv c_2,$$

$$c^E_{44} = c^E_{55} = c^E_{66} \equiv c_3,$$

$$p^E_{11} = p^E_{22} = p^E_{33} \equiv p_1,$$

$$p^E_{12} = p^E_{23} = p^E_{31} \equiv p_2,$$

$$p^E_{13} = p^E_{21} = p^E_{32} \equiv p_3,$$

$$p^E_{44} = p^E_{55} = p^E_{66} \equiv p_4.$$

The index S for the linear electro-optical effect tensor $\hat{r}^S$ means that the component r_{41} of the linear electro-optical effect tensor was measured for a clamped crystal; the components of the elasticity tensors $\hat{c}^E$ and the photoelastic effect $\hat{p}^E$ were measured at a constant electric field. The parameters n_1, n_2, n_3 are the direction cosines of the wave vector K_{hu} of the grating hu in the crystallographic coordinate system. In the above expressions, the tensor $\hat{\gamma}$ is the inverse of the tensor $\hat{\Gamma}$ with components: $\Gamma^E_{ik} = c^E_{ijkl} n_j n_l$, where c^E_{ijkl} — components of the elasticity tensor $\hat{c}^E$.

A distinctive feature of the above coupled wave equations from those presented earlier (see, for example, [7,19]) is that they have a fairly large generality, since the case was considered when they were obtained when six gratings with a phase-amplitude structure are simultaneously recorded in a dynamic mode during diffraction and mixing of light beams in an optically active piezoelectric absorbing medium. A wider range of issues related to the reconstruction and amplification of the wavefront scattered by an object, as well as the generation of optical radiation by lasers on dynamic gratings, can be considered using the presented theoretical model.

Let us consider the special case when the unit vectors of the orthonormal basis ($\mathbf{e}_1$, $\mathbf{e}_2$, $\mathbf{e}_3$) are oriented along crystallographic axes of the form $\langle 100 \rangle$ (i.e. $\theta = 0°$): $\mathbf{e}_1 \parallel [100]$, $\mathbf{e}_2 \parallel [010]$, $\mathbf{e}_3 \parallel [001]$. We will take into account the diffraction contributions of only secondary gratings when determining the efficiency of the WFC. We will assume in our calculations that the electric field strength of the gratings E_{sc} is 2 kV/cm, and the coupling coefficient characterizing the mixing of beams on amplitude gratings is $20\,\mathrm{m}^{-1}$. Let us use the material parameters of the BSO crystal borrowed from Ref. [23–25]: refractive index of an undisturbed crystal $n_0 = 2.54$ at $\lambda = 633 \cdot 10^{-9}$ m [23]; electro-optical coefficient $r_{41} = -5 \cdot 10^{-12}$ m/V [23]; elasticity coefficients $c_1 = 12.96 \cdot 10^{10}\,\mathrm{N/m^2}$, $c_2 = 2.99 \cdot 10^{10}\,\mathrm{N/m^2}$, $c_3 = 2.45 \cdot 10^{10}\,\mathrm{N/m^2}$ [24]; photoelasticity coefficients $p_1 = -0.16$, $p_2 = -0.13$, $p_3 = -0.12$, $p_3 = -0.015$ [25]; piezoelectric coefficient $e_{14} = 1.12\,\mathrm{C/m^2}$ [24]. The values of the specific rotation, absorption and circular dichroism of the crystal are assumed, respectively, to be $\rho = 384$ rad/m, $\chi = 1.5\,\mathrm{m}^{-1}$ and $\alpha = 15\,\mathrm{m}^{-1}$. Let us consider the intensity of the pump beams to be the same, besides their ratio to the intensity of the signal beam is 1:20. The angles φ_j in the crystal are chosen to be 5°.

The azimuths of beams 1 and 3 at the input to the crystal ($z = 0$) are assumed to be equal to each other ($\psi_1 = \psi_3 = \psi$) in calculations, and the input azimuth of the polarization of beam 2 for $z = d$ is found in accordance with the condition $\psi_2 = -\psi + \rho d$. The vectors E_1 and E_2 of the pump beams propagating inside the crystal ($0 < z \leq d$) remain parallel to each other if this condition is met. This choice of input azimuths of polarizations is attributable to the fact that the initial modulation depth of the interference patterns induced in the crystal will be optimal in this case [26]. We assume that the phase gratings recorded in the photorefractive crystal and the phase components of the mixed gratings are spatially displaced relative to the corresponding interference patterns by a quarter of the period ($\delta_{hu} = \pi/2$). The case when the spatial shift δ_{34} is $-\pi/2$ will be considered separately. All amplitude gratings recorded in a nonlinear medium, as well as the amplitude components of mixed gratings, are considered unbiased, as a result of which the parameter ϕ_{hu} is assumed to be zero.

The well-known [27] shooting method was used to numerically integrate the coupled wave equations. The initial conditions $E_{jp}(z)$ and $E_{js}(z)$ for the two-point boundary value problem were chosen as follows: $E_{1p}(0) = E_1 \cos\psi_1$, $E_{1s}(0) = E_1 \sin\psi_1$, $E_{2p}(d) = E_2 \cos\psi_2$, $E_{2s}(d) = E_2 \sin\psi_2$, $E_{3p}(0) = E_3 \cos\psi_3$, $E_{3s}(0) = E_3 \sin\psi_3$, $E_{4p}(d) = 0$, $E_{4s}(d) = 0$. The polarization components E_{4p} and E_{4s} were found at $z = 0$ as a result of solving the coupled wave equations. The efficiency of the WFC was evaluated using the reflectance R which is determined by the ratio of the intensity of the phase-conjugated beam at the exit from the crystal to the initial intensity of the signal beam [23]: $I_4(0)/I_3(0)$, where $I_3(0)$ and $I_4(0)$ — the intensities of the signal and phase-conjugated beams.

2. Results and discussion

Let's analyze the dependency graphs presented in Fig. 2 $R^{\max}(d)$ and $R^{\min}(d)$, which represent the envelopes of the maximum $R^{\max}$ (curves *1* and *2*) and minimum $R^{\min}$ (curves *3* and *4*) reflectance values calculated for the interval $0 < d \leq 20$ mm. The curves *2* and *3* are obtained for the case when the secondary gratings recorded in the crystal at FWM have only a phase structure, and the curves *1* and *4* are phase-amplitude. If the secondary gratings are amplitude, then the reflectance is practically independent of the polarization azimuth ψ and the graphs $R^{\max}(d)$, $R^{\min}(d)$ degenerate into a dependence $R(d)$(curve *5*). The method of finding the values of $R^{\max}$ and $R^{\min}$ at a fixed crystal thickness consists in using the following procedure. We

iterate over the values of the polarization azimuth ψ in increments of 2° in the range from 0 to 180° for each d, we find p- and s-components of light beams, numerically solve the system of coupled wave equations and determine the reflectances R. Next, we select the maximum $R^{\max}$ and minimum $R^{\min}$ values from the resulting series of values R. The parameter $R^{\max}$ is the azimuth-optimized value of the reflectance R. The value $R^{\min}$ will be useful in the future for analyzing the diffraction contributions of the phase and amplitude components of the gratings when studying the efficiency of the WFC. The term „diffraction contribution" will be understood as the percentage ratio of the intensity of the diffracted beam formed by one of the components (phase or amplitude) of the mixed grating to the total intensity of the phase-conjugated beam.

Let us first consider the hypothetical case of recording only amplitude gratings in a crystal. This situation can be realized, for example, when recording a transmission grating with a wave vector parallel to the crystallographic axis [100]. The amplitude of the refractive index modulation will be approximately zero due to the anisotropy of the linear electro-optical effect, and the transmission grating can be recorded by modulating the absorption coefficient of the crystal. The intensity of the phase-conjugated beam increases monotonously with the increase of the crystal thickness and at $d = 20$ mm the gain is $R = 3.2 \cdot 10^{-3}$ in the case of recording of amplitude gratings 14, 24 and 34 as can be seen from Fig. 2. It can be argued that the diffraction contribution of the amplitude component of the grating in thin BSO crystals will also be quite small due to the relatively small values of R. However, the optical activity results in a decrease of the intensity of the phase-conjugated beam formed during beam diffraction on the phase grating

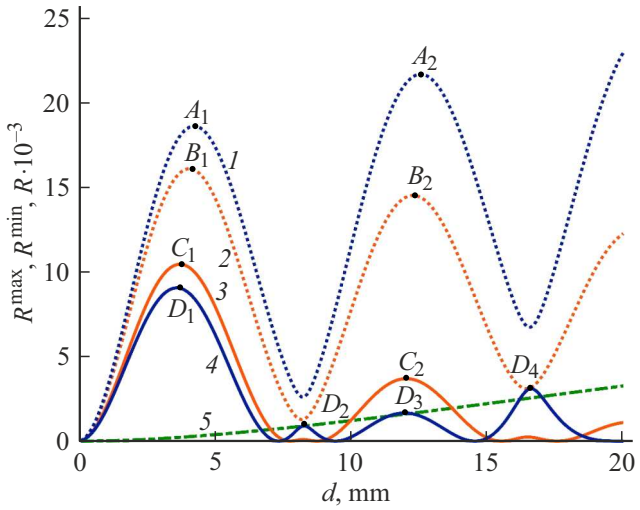

Figure 2. Envelopes of maximum (curves *1* and *2*) and minimum (curves *3* and *4*) reflectance values calculated for phase (curves *2* and *3*) and mixed (curves *1* and *4*) gratings 14, 24, 34 with spatial shifts $\delta_{14} = \delta_{24} = \delta_{34} = \pi/2$; dependence of the reflectance R on the thickness d (curve *5*), calculated for unbiased amplitude gratings 14, 24, 34.

at some values of d, and in these cases the efficiency of the WFC will be determined by the diffraction contribution of the amplitude grating.

The graph of dependence $R^{\max}(d)$ has a periodic character (curve *2* in Fig. 2) when phase gratings are formed in a crystal, which is attributable to the effect of optical activity. The local maxima of the reflectance, which are indicated in Fig. 2 by the points B_1 and B_2, are achieved at such values d, for which the angle of rotation of the polarization plane of the light beams propagating in the crystal is 90° and 270°, which corresponds quite accurately to the expression $d = w\pi/(2\rho)$ $(w = 1,\ 3)$: B_1 — $d = 4.1$ mm, B_2 — $d = 12.3$ mm. The values of $R^{\max}$ in local maxima decrease with the increase of the crystal thickness: $R^{\max} = 16.1 \cdot 10^{-3}$ (point B_1) and $R^{\max} = 14.5 \cdot 10^{-3}$ (point B_2), which can be explained by the effect of crystal absorption and destructive interference of diffracted waves formed during diffraction on phase gratings. The comparison of the curves *2* and *5* can demonstrate that the azimuth-optimized polarization value of the reflectance $R^{\max}$ obtained for phase gratings for any value d will exceed the reflectance R obtained for amplitude gratings.

It can be seen when considering the dependence graph $R^{\min}(d)$ (curve *3* in Fig. 2) that the maximum gain values at points C_1 $(R^{\min} = 10.1 \cdot 10^{-3})$, C_2 $(R^{\min} = 3.7 \cdot 10^{-3})$ decrease with the increase of d. The local maxima of the dependence graph $R^{\min}(d)$ correspond to smaller thickness values than in the dependence graph $R^{\max}(d)$: C_1 — $d = 3.7$ mm, C_2 — $d = 12$ mm. The comparison of the curves *3* and *5* can demonstrate that the gain achieved during recording of phase gratings in the crystal will be greater than in case of recording of the amplitude gratings in the intervals $0 \le d \le 7.1$ mm and $10 < d \le 13.7$ mm for any value of the polarization azimuth ψ. The diffraction on amplitude gratings can achieve a higher intensity of the phase-conjugated beam than on phase gratings for the remaining thickness values in the range $0 < d \le 20$ mm.

The diffraction efficiency will have the highest value if mixed gratings are recorded in the crystal, since the maximum possible value of $R^{\max}$ is achieved for gratings with a phase-amplitude structure for any fixed value of d (Fig. 2). The fundamental difference between the dependencies $R^{\max}(d)$ obtained for mixed (curve *1*) and phase gratings (curve *2*) is that the gain values in the local maxima of the graph $R^{\max}(d)$ calculated for the mixed grating, increase with increasing crystal thickness: point A_1 — $R^{\max} = 18.6 \cdot 10^{-3}$, point A_2 — $R^{\max} = 21.7 \cdot 10^{-3}$. This can be explained by the fact that when choosing the optimal polarization azimuth ψ , the decrease of $R^{\max}$ characteristic of phase gratings with the increase of thickness is compensated by adding the diffraction contribution of the amplitude components of the mixed gratings, which increases with the increase of d. Local maxima on the curve *1* are slightly offset along the abscissa axis towards the increase of the values of d relative to the points B_1 and B_2 on the curve *2*: the first maximum (point A_1) of

the curve *1* is reached at $d = 4.3$ mm and corresponds to the angle of rotation $\rho d = 95°$, and the second maximum (point A_2) is located at $d = 12.6$ mm, for which the angle of rotation ρd is 277°. This is attributable to the fact that the intensity of the phase-conjugated beam in the case of recording mixed gratings is maintained by the diffraction contribution of their amplitude components with an increase of d after the points B_1 and B_2 corresponding to the local maxima $R^{\max}$ for phase gratings. The local maxima A_1 and A_2 are shifted relative to the points B_1 and B_2 only by a few millimeters since the intensities of the phase-conjugated beams generated by phase and amplitude gratings differ almost tenfold with such thicknesses. Thus, when mixed gratings are formed in a crystal, the conditions for achieving the highest diffraction efficiency change relative to the case of recording phase gratings: the values of the reflectance R optimized by azimuth of polarization increase and the values of the crystal thickness at which local maxima of the graph of dependence $R^{\max}(d)$ are reached change.

The local maxima of the graph of dependence $R^{\min}(d)$ calculated for mixed gratings (curve *4*) are reached at points D_1 ($d = 3.6$ mm), D_2 ($d = 8.2$ mm), D_3 ($d = 12$ mm) and D_4 ($d = 16.4$ mm). The points D_1 and D_3 correspond to such values d that lie in the vicinity of $d = w\pi/(2\rho)$ ($w = 1, 3$), and the thickness values at which the local maxima D_2 and D_4 occur, meet the following condition fairly accurately: $d = w\pi/(2\rho)$ ($w = 2, 4$). The highest value $R^{\min}$ is reached at the point D_1 ($R^{\min} = 9.1 \cdot 10^{-3}$), and it has the maximum possible value in the range of $0 < d \leq 20$ mm, because of the destructive effect of optical activity on the intensity of the phase-conjugated beam formed at diffraction on the phase components of the gratings. The remaining local maxima of the graph of dependence $R^{\min}(d)$ correspond to the following values of the reflectance: D_2 — $R^{\min} = 0.9 \cdot 10^{-3}$, D_3 — $R^{\min} = 1.6 \cdot 10^{-3}$ and D_4 — $R^{\min} = 3.1 \cdot 10^{-3}$. The increase of the values of $R^{\min}$ at the points D_2, D_3 and D_4 is associated with an increase of the diffraction contribution of the amplitude components of the gratings. Local maxima D_1, D_2, D_3 and D_4 are achieved when the electric field strength vectors of beams 1 and 3 are oriented relative to the plane of incidence at an angle $\psi = 67°$. Obviously, the azimuth values ψ_2 for the points D_1, D_2, D_3 and D_4 will significantly differ from each other due to the high specific rotation of the crystal because of the fulfillment of equality: $\psi_2 = -\psi + \rho d$. It should be noted that the results obtained cannot be used to find optimal azimuth values at which the highest diffraction efficiency is achieved in a photorefractive crystal with $\bar{4}3m$ symmetry class, since optical activity results in the appearance of a complex of polarization phenomena during the mixing of light beams on gratings in crystals of 23 symmetry class and changes of optimal mixing conditions relative to semiconductor crystals [26].

Let us consider the physical mechanism of diffraction of light beams on phase gratings at FWM in a crystal of 23 symmetry class of (001)-cut if the condition $d = w\pi/(2\rho)$ ($w = 1, 2, \ldots$) is fulfilled. For such a holographic configuration the largest diffraction contribution in the formation of an phase-conjugated beam among the phase components of the gratings 14, 24 and 34 is made. For such a holographic configuration by a reflection grating 14, whose wave vector is directed along the crystallographic direction [001]. It follows from the solution of the equations of the Fresnel's normals that the when recording such a grating BSO crystal becomes optically anisotropic and main axes of the section of the optical indicatrix of BSO crystal correspond to the refractive indices $n_{1,2} = n_0 \pm \Delta n$, where $\Delta n = n_0^3 r_{41} E_{sc}/2$, where $n_{1,2}$ — refractive indices of its normal waves [26]. The diffracted waves occurring in the crystal are polarized in mutually perpendicular directions and shifted in phase by π. The phase-conjugated beam will amplify in case of polarization along one of the main axes of the section due to coherent addition with a diffracted wave, and it will weak in case of polarization along the second main axis [26]. The rotation angle of the polarization plane of the light beams is 90° ($w = 1$) and 270° ($w = 3$) when the condition $d = w\pi/(2\rho)$ ($w = 1, 3$) is met. This means that at such values d, in the case of an optimal choice of azimuth ψ, the intensity vectors of the electric fields of the beams will be oriented closer to the main axis along which the phase-conjugated beam will be amplified, resulting in the highest reflectances. This is the main reason for the location of all local maxima in Fig. 2 in the vicinity of $d = \pi/(2\rho)$ (4.1 mm) and $d = 3\pi/(2\rho)$ (12.3 mm) with the exception of points D_2, D_4 for which the existence of a local maximum is attributable to the diffraction contribution of the amplitude component of the grating. The rotation angles of the polarization planes of the light beams are 180° ($w = 2$) and 360° at $w = 2, 4$ ($w = 4$). This means that the intensity vectors of the electric fields of the beams propagating in the crystal for any azimuth value ψ will be oriented half way closer to the main axis, along which the coherent addition of the phase-conjugated beam with the diffracted wave occurs, and half way — closer to the main axis, along which the phase-conjugated beam and the diffracted wave is subtracted. The diffraction efficiency on the phase component of the grating is close to zero as a result. This explains that the diffraction contribution of the phase components of the mixed gratings is relatively small at $d = \pi/\rho$ (8.2 mm) and $d = 2\pi/\rho$ (16.4 mm).

The comparison of the dependencies $R^{\min}(d)$ (curves *3* and *4*) and $R(d)$ (curve *5*) demonstrates that the highest values of $R^{\min}$ are achieved in the intervals $0 \leq d \leq 7.1$ mm and $10\,\text{mm} < d \leq 13.7$ mm under the condition of formation of phase gratings in the crystal. The gain of the amplitude gratings in intervals $7.1\,\text{mm} < d \leq 10$ mm, $13.7\,\text{mm} < d \leq 16.2$ mm and $17\,\text{mm} < d \leq 20$ mm exceeds the values $R^{\min}$ corresponding to phase and mixed gratings. The diffraction contribution of the phase components of the gratings is approximately zero at $d = \pi/(2\rho)$ and $R^{\min}$ for mixed gratings matches the gain of the amplitude gratings ($R^{\min} = R$). The highest values of reflectance are achieved

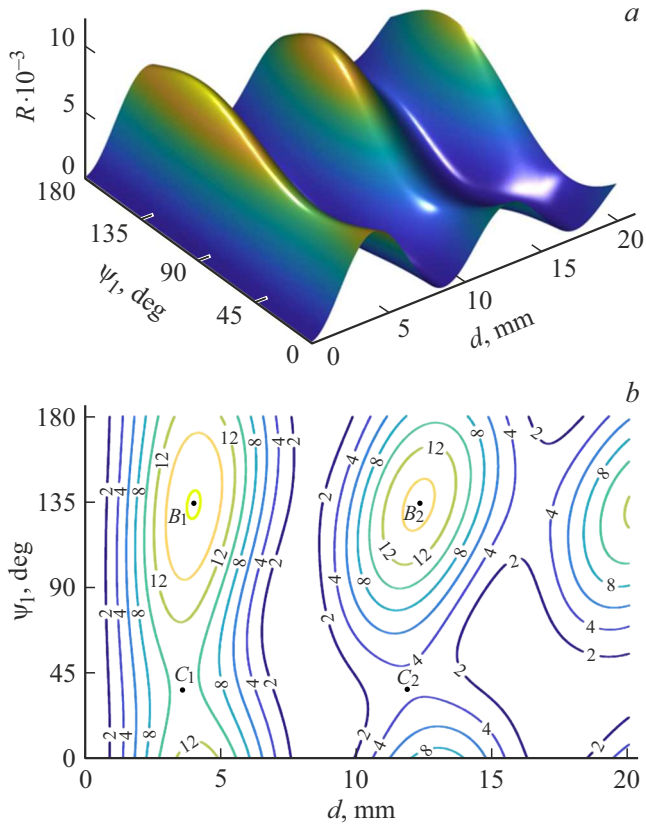

Figure 3. Dependence of the reflectance on the azimuth of polarization ψ and thickness d, calculated for phase gratings 14, 24, 34 with spatial shifts $\delta_{14} = \delta_{24} = \delta_{34} = \pi/2$ and presented as a surface (a) and contour graph (b).

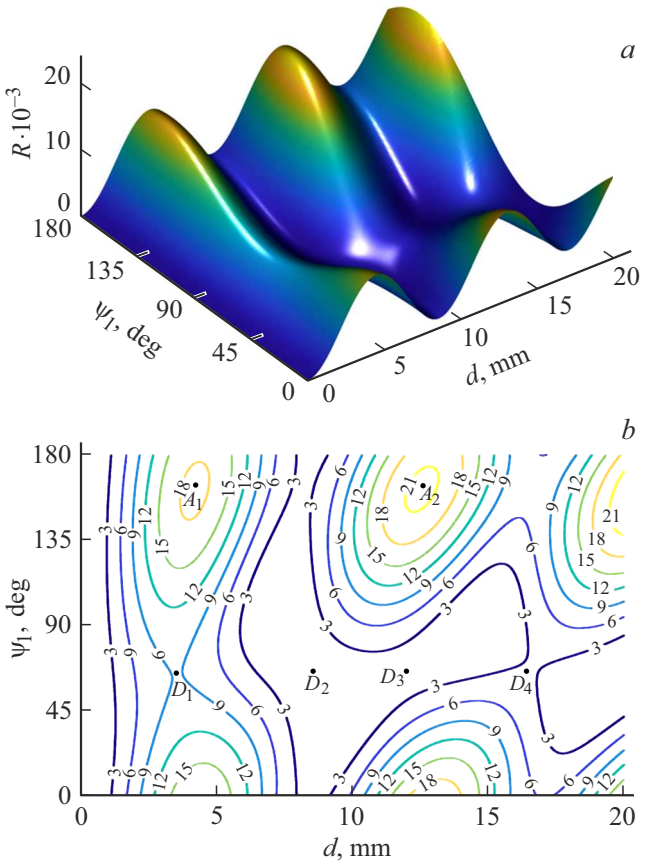

Figure 4. Dependence of the reflectance on the azimuth of polarization ψ and thickness d, calculated for mixed gratings 14, 24, 34 with spatial shifts $\delta_{14} = \delta_{24} = \delta_{34} = \pi/2$ and presented as a surface (a) and contour graph (b).

in the range of $16.2\,\text{mm} < d \leq 17\,\text{mm}$ in case of recording of mixed gratings in a BSO crystal.

Fig. 2 shows that the values of the reflectance can vary quite broadly in the case of recording phase or mixed gratings in a BSO crystal. For this reason let us consider the question of finding the optimal values of the polarization azimuths ψ, at which the mode of maximum efficiency of the WFC is realized. Figures 3 and 4 show graphs of dependencies $R(d, \psi)$ calculated for phase (Fig. 3) and mixed gratings (Fig. 4), which are wavelike surfaces with pronounced maxima. The highest values of the gain for the phase gratings marked with points B_1 and B_2 in the graph $R^{\max}(d)$ (Fig. 2) are achieved at $\psi = 135°$. Such an azimuth of polarization corresponds to the orientation of the intensity vectors of the pump and signal light beams at the input to the crystal along the $\langle 110 \rangle$ crystallographic direction. The local maxima of the dependence $R^{\min}(d)$ marked on the surface $R(d, \psi)$ by the points C_1 and C_2 are located at $\psi = 40°$. The position of the local maxima of the surface $R(d, \psi)$ corresponding to the points A_1 and A_2 changes to 27° at the coordinate ψ in case of recording mixed gratings in a crystal and is equal to 162°. A similar change of the values of ψ also occurs for the local maxima of the dependence $R^{\min}(d)$ shown in Fig. 2, since the points D_1, D_2, D_3 and D_4 approximately correspond to $\psi = 67°$ (Fig. 4, b) Therefore, the difference of the values of the polarization azimuths at which the local maxima of the dependencies $R^{\max}(d)$ and $R^{\min}(d)$ obtained for phase and mixed gratings are reached is 27°. This may be associated with the peculiarities of diffraction of light beams on phase and amplitude gratings in an optically active medium. The phase gratings formed in the BSO crystal of (001)-cut are optically anisotropic, and the diffraction efficiency depends on the initial values of the polarization azimuths of the entering light beams (see, for example, [28]), and the amplitude gratings are optically isotropic, and the rotation of the polarization plane of the light beams does not significantly affect the reflectance. Simultaneous diffraction of light beams on optically isotropic and anisotropic gratings in case of FWM occurs on mixed holograms, which results in a transformation of the surface $R(\psi, d)$ and a change of the optimal values of the polarization azimuth ψ.

The mutual spatial shift of the photorefractive gratings recorded in the crystal is a key factor determining the occurrence of „positive feedback“ and the WFC efficiency [3]. Let us study the patterns of the effect of spatial shift on the dependence of the reflectance on the thickness d and

the azimuth of polarization ψ by considering a special case when the parameter δ_{34} changes from $\pi/2$ to $-\pi/2$. A similar problem for phase gratings in a BSO crystal was considered in sufficient detail in Ref. [18]. The comparison of Fig. 2 and 5 demonstrates that the change of the parameter δ_{34} to π for any thickness value in the range of $0 < d \leq 20$ mm results in an almost halving of the values $R^{\max}$ for phase and mixed gratings. For example, the values of $R^{\max}$ achieved at $\delta_{34} = \pi/2$ at points A_1, A_2 decrease by $9.7 \cdot 10^{-3}$ for mixed gratings and they are equal to $R^{\max} = 8.8 \cdot 10^{-3}$ (point E_1) and $R^{\max} = 12 \cdot 10^{-3}$ (point E_2), accordingly, for $\delta_{34} = -\pi/2$. The difference between the values of $R^{\max}$ for phase gratings at local maxima B_1, B_2 in Fig. 2 and F_1, F_2 in Fig. 5 is approximately equal to $7.9 \cdot 10^{-3}$. A decrease of the azimuth-optimized polarization values of the reflectance in case of a change of the sign of the spatial shift δ_{34} indicates a change of the beam diffraction mode on the secondary gratings, which results in a subtraction of the diffraction contributions of the gratings 14, 24 and 34.

A decrease of the diffraction contribution of the phase components of the gratings when the sign of the spatial shift δ_{34} is reversed also results in a change of the reflectance in the local maxima of the dependence $R^{\min}(d)$ (Fig. 2 and 5). The value of $R^{\min}$ decreases more than three times to $2.9 \cdot 10^{-3}$ (point H_1) with $d = \pi/(2\rho)$, and the intensity of the phase-conjugated beam is almost zero with $d = 3\pi/(2\rho)$. However, the values of $R^{\min}$ at points D_2, H_2 and D_4, H_4 are approximately equal in the vicinity of $d = w\pi/(2\rho)$ $(w = 2, 4)$. The comparison of the curves $3-5$ in Fig. 5 demonstrates that the largest values of $R^{\min}$ are achieved in the range of $0 \leq d \leq 6.4$ mm when

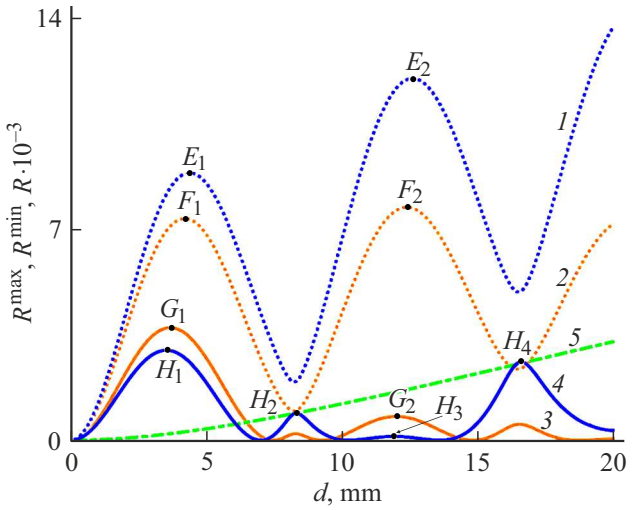

Figure 5. Envelopes of maximum (curves *1* and *2*) and minimum (curves *3* and *4*) reflectance values calculated for phase (curves *2* and *3*) and mixed (curves *1* and *4*) gratings 14, 24, 34 with spatial shifts $\delta_{14} = \delta_{24} = \pi/2$, $\delta_{34} = -\pi/2$; dependence of the reflectance R on thickness d (curve *5*) calculated for unbiased amplitude gratings 14, 24, 34.

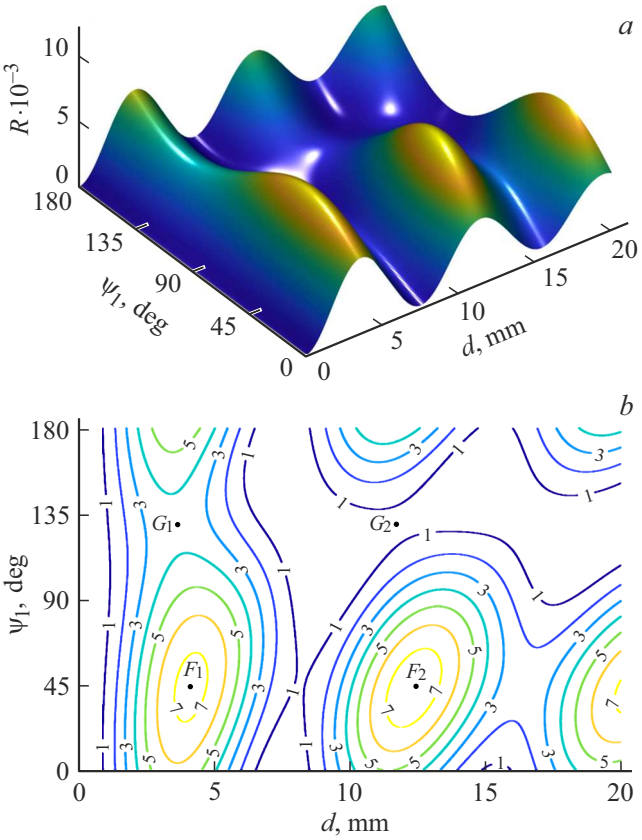

Figure 6. Dependence of the reflectance on the azimuth of polarization ψ and thickness d, calculated for mixed gratings 14, 24, 34 with spatial shifts $\delta_{14} = \delta_{24} = \pi/2$, $\delta_{34} = -\pi/2$ and presented as a surface (a) and a contour graph (b).

recording phase gratings, and for the remaining thickness values — amplitude gratings.

It follows from the comparison of Fig. 3, 4 with Fig. 6, 7 that the local maxima of the dependence graphs $R^{\max}(d, \psi)$ are shifted by the values of the azimuth of polarization by approximately 90° when the sign of the phase shift δ_{34} is reversed. When recording of phase gratings at $\delta_{34} = -\pi/2$, the highest values of the reflectance are achieved at azimuth 45° (points F_1 and F_2 in Fig. 6, b), which differs by Δ from the value ψ corresponding to the points B_1 and B_2 in Fig. 3, b. A similar situation is observed when recording mixed gratings: the highest values of the reflectance achieved at $\delta_{34} = \pi/2$ for the polarization azimuth $\psi = 162°$ (points A_1 and A_2 in Fig. 4, b), at $\delta_{34} = -\pi/2$ correspond to $\psi = 72°$ (points E_1 and E_2 in Fig. 7, b). The polarization azimuths corresponding to the local maxima of the dependence $R^{\min}(d)$ also change by 90° for both phase and mixed gratings.

Conclusion

A system of coupled wave equations is obtained that is suitable for finding the vector amplitudes of linearly

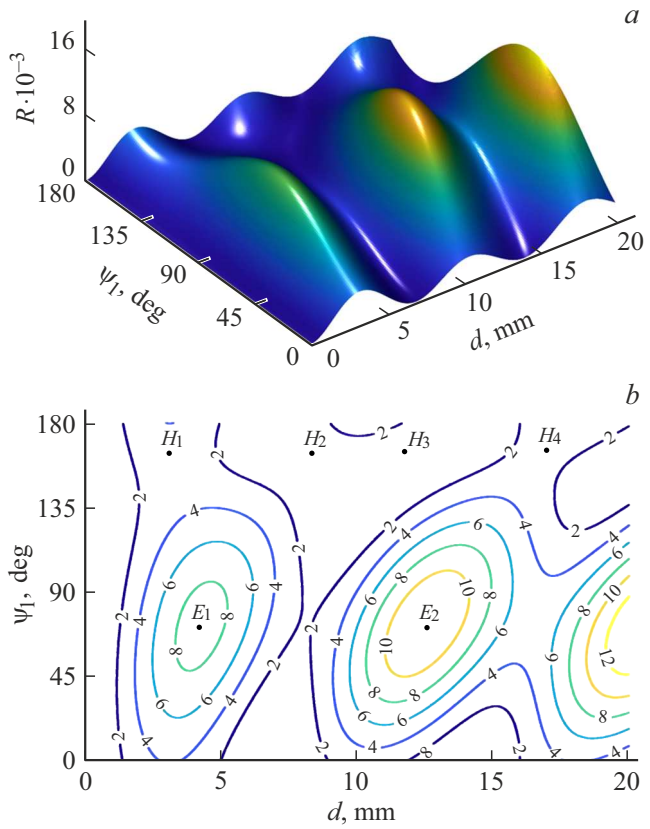

Figure 7. Dependence of the reflectance on the azimuth of polarization ψ and thickness d, calculated for mixed gratings 14, 24, 34 with spatial shifts $\delta_{14} = \delta_{24} = \pi/2$, $\delta_{34} = -\pi/2$ and presented as a surface (a), and a contour graph (b).

polarized light beams with an contra-directional degenerate FWM in a cubic photorefractive crystal. The consideration of the phase-amplitude structure of holographic gratings recorded in a nonlinear medium is a distinctive feature of the obtained mathematical model distinguishing it from the previously known models. When deriving the equations, it was assumed that three primary mixed gratings are formed in the crystal as a result of the interaction of the pump and signal beams, and a secondary recording of three mixed gratings takes place when these beams interfere with the phase-conjugated beam. The conditions for achieving the highest diffraction efficiency in FWM were studied by assuming in the theoretical model that the spatial shifts of the mixed gratings relative to the corresponding interference patterns have arbitrary values.

The efficiency of diffraction at FWM in a cubic photorefractive crystal depends on the structure of the recorded dynamic gratings and can be increased by an appropriate choice of crystal thickness and the input azimuth of polarization of light beams. The reflectance achieved for mixed gratings will be greater than for phase gratings in the case of an optimal choice of the polarization azimuth for any thickness value in the range $0 < d \leq 20$ mm. The diffraction contributions of the phase and amplitude components of the mixed grating can be subtracted for the remaining values of the polarization azimuth, and the reflectance achieved for it will be less than the reflectance for the phase grating. If the crystal thickness is in the vicinity of $d = w\pi/\rho$ $(w = 1, 3, \ldots)$, then the diffraction contribution of the phase component of the grating is practically zero with any azimuth of polarization and the intensity of the phase-conjugated beam is determined by the diffraction efficiency on its amplitude component. The values of the crystal thickness, which correspond to the local maxima of the dependence of the azimuth-optimized polarization values of the reflectance, for mixed and phase gratings are approximately equal to each other. At the same time, the values of the polarization azimuth, for which the maximum values of the phase-conjugated beam intensity for mixed and phase gratings are achieved, differ by 27°, which is attributable to the diffraction contribution of the amplitude component of the mixed grating.

The values of the crystal thickness and the input azimuth of the polarization of light beams, at which the highest values of the reflectance $R^{\max}$ are achieved, depend on the magnitude of the spatial shift of the phase and mixed gratings relative to the interference pattern induced in the crystal. It is shown using the example of the reflection grating 34 that a change of the spatial shift from $\pi/2$ to $-\pi/2$ can result in an almost twofold decrease of the values in the local maxima of the dependence of the reflectance values optimized by azimuth of polarization of light beams. At the same time, the values of the polarization azimuths at which the maximum intensity of the phase-conjugated beam is achieved, change by 90° for both mixed and phase gratings.

The results obtained can be used for the selection of conditions for a holographic experiment (crystal thickness, polarization of light beams, orientation of the wave vectors of holographic gratings relative to the crystallographic axes of the recording medium) to increase the efficiency of diffraction in devices using photorefractive crystals.

Funding

The study was financially supported by the Ministry of Education of the Republic of Belarus (agreement dated March 22, 2021 №1410/2021) within the State Program of Scientific Studies №6 „Photonics and Electronics for Innovations“ in 2021–2025 (assignment 1.01.14).

Acknowledgment

I would like to express my gratitude to the reviewers for a thoughtful and attentive reading of the manuscript of the article, as well as for useful comments, which contributed to improving the scientific level and content of the paper.

Conflict of interest

The author declares that he has no conflict of interest.

References

[1] G. Montemezzani, M. Zgonik. Phys. Rev. E, **55** (1), 1035 (1997). DOI: 10.1103/PhysRevE.55.1035

[2] K. Shcherbin, S. Odoulov, R. Litvinov, E. Shandarov, S. Shandarov. J. Opt. Soc. Am. B, **13** (10), 2268 (1996). DOI: 10.1364/JOSAB.13.002268

[3] S.G. Odulov, M.S. Soskin, A.I. Khizhnyak. *Lazery na dinamicheskikh reshetkakh: opticheskie generatory na chetyrekhvolnovom smeshenii* (Nauka, M., 1990) (in Russian).

[4] P.M. Petersen, P.M. Johansen. Opt. Lett., **13** (1), 45 (1988). DOI: 10.1364/OL.13.000045

[5] Y. Ding, H.J. Eichler Opt. Comm., **110**, 456 (1994). DOI: 10.1016/0030-4018(94)90449-9

[6] S.I. Stepanov, V.M. Petrov. Opt. Comm., **53**, 64 (1985). DOI: 10.1016/0030-4018(85)90263-9

[7] A. Erdmann, R. Kowarschik. IEEE J. Quant. Electron., **24** (2), 155 (1988). DOI: 10.1109/3.109

[8] V.V. Shepelevich. J. Appl. Spectr., **78** (4), 461 (2011). DOI: 10.1007/s10812-011-9487-9

[9] B.I. Stepanov, E.V. Ivakin, A.S. Rubanov. Dokl. Akad. Nauk SSSR, **196** (3), 567 (1971) (in Russian).

[10] I.G. Dadenkov, A.L. Tolstik, Yu.I. Miksyuk, K.A. Saechnikov. Opt. Spectr., **128** (9), 1401 (2020). DOI: 10.1134/S0030400X20090052

[11] A.L. Tolstik, E.V. Ivakin, I.G. Dadenkov. J. Appl. Spectr., **90**, 407 (2023). DOI: 10.1007/s10812-023-01547-1

[12] S.M. Shandarov, V.M. Shandarov, A.E. Mandel, N.I. Burimov. *Fotoreaktivnye effekty v elektroopticheskikh kristallakh* (TUSUR, Tomsk, 2012) (in Russian).

[13] R.V. Litvinov, S.I. Polkovnikov, S.M. Shandarov. Quant. Electron., **31** (2), 167 (2001). DOI: 10.1070/QE2001v031n02ABEH001911

[14] A.V. Gusel'nikova, S.M. Shandarov, A.M. Plesovskikh, R.V. Romashko, Yu.N. Kulchin. J. Opt. Technol., **73** (11), 760 (2006). DOI: 10.1364/JOT.73.000760

[15] M.A. Bryushinin, V.V. Kulikov, I.A. Sokolov, E.N. Savchenkov, N.I. Burimov, S.M. Shandarov, A.R. Akhmatkhanov, M.A. Chuvakova, V.Ya. Shur. Phys. Solid State, **65** (2), 200 (2023). DOI: 10.21883/PSS.2023.02.55400.519

[16] R.I. Anisimov, A.S. Temereva, A.A. Kolmakov, S.M. Shandarov. Opt. Spectr., 131 (10), 1298 (2023). DOI: 10.61011/EOS.2023.10.57759.5480-23

[17] V.M. Petrov, A.V. Shamray. *Interferentsiya i diffraktsiya dlya interferentsionnoy fotoniki* (Lan, SPb., 2019) (in Russian).

[18] V.N. Naunyka. Tech. Phys. Lett., **49** (10), 71 (2023).

[19] V.N. Naunyka. Opt. Spectr., **130** (3), 324 (2022). DOI: 10.21883/EOS.2022.03.53557.2936-21

[20] S.I. Stepanov, M.P. Petrov, M.V. Krasinkova. ZhTF, **54** (6), 1223 (1984) (in Russian).

[21] V.I. Burkov, Yu.F. Kargin, V.A. Kizel, V.I. Sitnikova, V.M. Skorikov. Pis'ma v ZhETF, **38** (7), 326 (1988) (in Russian).

[22] S.M. Shandarov, V.V. Shepelevich, N.D. Khatkov. Opt. Spectrosc., **70** (5), 627 (1991).

[23] M.P. Petrov, S.I. Stepanov, A.V. Knomenko. *Photorefraktivnye kristally v kogerentnoi optike* (Nauka, SPb., 1992) (in Russian).

[24] K.S. Alexandrov, V.S. Bondarenko, M.P. Zaitseva, B.P. Sorokin, Yu.I. Kokorin, V.M. Zrazhevsky, B.V. Sobolev. FTT, **26** (12), 3603 (1984) (in Russian).

[25] G.A. Babonas, A.A. Reza, E.I. Leonov, V.I. Shandaris. ZhTF, **55** (6), 1203 (1985) (in Russian).

[26] S. Mallick, M. Miteva, L. Nikolova. J. Opt. Soc. Am. B, **14** (5), 1179 (1997). DOI: 10.1364/JOSAB.14.001179

[27] Y.H. Ja. Opt. Quant. Electron., **15**, 539 (1983). DOI: 10.1007/bf00620022

[28] V.N. Naunyka, V.V. Shepelevich. Tech. Phys. Lett., **99** (9), 726 (2007). DOI: 10.1134/S1063785007090039

Translated by A.Akhtyamov